J|A|C|S
ARTICLES
Published on Web 04/10/2007

Secretory Phospholipase A_2 Hydrolysis of Phospholipid Analogues Is Dependent on Water Accessibility to the Active Site

Günther H. Peters,*,† Martin S. Møller,† Kent Jørgensen,§ Petra Rönnholm,§ Mette Mikkelsen,§ and Thomas L. Andresen*,‡,§

Contribution from the Department of Chemistry, MEMPHYS-Center for Biomembrane Physics, Technical University of Denmark, DK-2800 Lyngby, Denmark, Risø National Laboratory, Technical University of Denmark, 4000 Roskilde, Denmark, and LiPlasome Pharma A/S, Technical University of Denmark, DK-2800 Lyngby, Denmark

Received October 30, 2006; E-mail: thomas.andresen@risoe.dk

Abstract: A new and unnatural type of phospholipids with the head group attached to the 2-position of the glycerol backbone has been synthesized and shown to be a good substrate for secretory phospholipase A_2 ($sPLA_2$). To investigate the unexpected $sPLA_2$ activity, we have compared three different phospholipids by using fluorescence techniques and HPLC, namely: (*R*)-1,2-dipalmitoyl-glycero-3-phosphocholine (hereafter referred to as **1R**), (*R*)-1-*O*-hexadecyl-2-palmitoyl-glycero-3-phoshocholine (**2R**), and (*S*)-1-*O*-hexadecyl-3-palmitoyl-glycero-2-phosphocholine (**3S**). Furthermore, to understand the underlying mechanisms for the observed differences, we have performed molecular dynamics simulations to clarify on a structural level the substrate specificity of $sPLA_2$ toward phospholipid analogues with their head groups in the 2-position of the glycerol backbone. We have studied the lipids above **1R**, **2R**, and **3S** as well as their enantiomers **1S**, **2S**, and **3R**. In the simulations of $sPLA_2$−**1S** and $sPLA_2$−**3R**, structural distortion in the binding cleft induced by the phospholipids showed that these are not substrates for $sPLA_2$. In the case of the phospholipids **1R**, **2R**, and **3S**, our simulations revealed that the difference observed experimentally in $sPLA_2$ activity might be caused by reduced access of water molecules to the active site. We have monitored the number of water molecules that enter the active site region for the different $sPLA_2$−phospholipid complexes and found that the probability of a water molecule reaching the correct position such that hydrolysis can occur is reduced for the unnatural lipids. The relative water count follows **1R** > **2R** > **3S**. This is in good agreement with experimental data that indicate the same trend for $sPLA_2$ activity: **1R** > **2R** > **3S**.

Introduction

Cell membrane organization plays a prominent role in cell regulation, and the earlier picture of a cell membrane being a homogeneous mixture of lipids and proteins as suggested by the Singer and Nicholson model is now significantly revised.[1,2] A more complex picture involving membrane domains of different compositions and regions of varying curvatures has emerged that is believed to play important regulatory roles in for instance membrane trafficking, protein sorting, and formation of nanotubules.[2−4] Lipid rafts, hydrophobic mismatch, membrane phospholipid asymmetry, domain formation in membranes, and enzymatic restructuring of the membrane are a few examples of specific mechanisms by which membranes can take part in signal transduction events.[3,5−13]

Phospholipase A_2 enzymes (PLA_2s) are responsible for the remodeling of cellular phospholipids and the generation of intracellular messengers.[14−16] PLA_2s are a diverse class of hydrolytic enzymes that cleave the ester-linkage in the *sn*-2 position of aggregated glycerolphospholipids, yielding free fatty acids and lyso-phospholipids.[17−20] The PLA_2 superfamily includes the calcium-independent PLA_2, the high molecular

† Department of Chemistry, MEMPHYS-Center for Biomembrane Physics.
‡ Risø National Laboratory.
§ LiPlasome Pharma A/S.

(1) Singer, S. J.; Nicolson, G. L. *Science* **1972**, *175*, 720−731.
(2) Edidin, M. *Nat. Rev. Mol. Cell Biol.* **2003**, *4*, 414−418.
(3) Edidin, M. *Curr. Opin. Struct. Biol.* **1997**, *7*, 528−532.
(4) Brown, W. J.; Chambers, K.; Doody, A. *Traffic* **2003**, *4*, 214−221.
(5) Mouritsen, O. G. *Chem. Phys. Lipids* **1991**, *57*, 179−194.
(6) Kusumi, A.; Sako, Y. *Curr. Opin. Cell Biol.* **1996**, *8*, 566−574.
(7) Wisniewska, A.; Draus, J.; Subczynski, W. K. *Cell Mol. Biol. Lett.* **2003**, *8*, 147−159.
(8) Rieman, D.; Hansen, G. H.; Niels-Christiansen, L.-L.; Thorsen, E.; Immerdahl, L.; Santos, A. N.; Kehlen, A.; Langner, J.; Danielsen, E. M. *Biochem. J.* **2001**, *354*, 47−55.
(9) Caselli, A.; Mazzinghi, B.; Camici, G.; Manao, G.; Ramponi, G. *Biochem. Biophys. Res. Commun.* **2002**, *296*, 692−697.
(10) Zhuang, L.; Lin, J.; Lu, M. L.; Solomon, K. R.; Freeman, M. R. *Cancer Res.* **2002**, *62*, 2227−2231.
(11) Baron, G. S. *EMBO J.* **2002**, *21*, 1031−1040.
(12) Kakio, A.; Nishimoto, S.-I.; Yanagisawa, K.; Kozutsumi, Y.; Matsuzaki, K. *Biochemistry* **2002**, *41*, 7385−7390.
(13) Simons, K.; Ikonen, E. *Nature* **1997**, *387*, 569−572.
(14) Leistad, L.; Feuerherm, A. J.; Østensen, M.; Faxvaag, A.; Johansen, B. *Clin. Chem. Lab. Med.* **2004**, *42*, 602−610.
(15) Leidy, C.; Mouritsen, O. G.; Jørgensen, K.; Peters, G. H. *Biophys. J.* **2004**, *87*, 408−418.
(16) Leidy, C.; Kaasgaard, T.; Mouritsen, O. G.; Jørgensen, K.; Peters, G. H. *Recent Res. Devel. Biophys.* **2004**, *3*, 163−185.
(17) Six, D. A.; Dennis, E. A. *Biochim. Biochim. Acta* **2000**, *1488*, 1−19.

weight cytosolic PLA_2, and the low molecular weight secretory PLA_2 ($sPLA_2$).[17,21] Further classifications are based on their source, subcellular location, calcium requirements, amino acid similarity, and number of disulfide bridges.[17,20] The activity of $sPLA_2$ depends strongly on the physical state and microstructure of the membrane surface,[15,16,22−26] and it has been recognized that differential binding of mammalian $sPLA_2$ to membranes of different phospholipid compositions has physiological significance.[27,28] For instance, human tear fluid contains a high concentration of human $sPLA_2$-IIA as a protection against bacterial infection.[29,30] Human $sPLA_2$-IIA does not degrade the outer plasma membrane of a number of mammalian cells, which are rich in zwitterionic lipids (phosphocholines; PC),[31−33] but the enzyme is able to degrade cell membranes of Gram-positive bacteria that contain high levels of anionic lipids.[23,34] The observed increased activity in the presence of anionic lipids is a general feature of $sPLA_2$s[23,35−37] and might be governed by electrostatic interactions between charged residues located at the binding surface of the enzyme and charged head groups of the phospholipids.[35,38] However, many $sPLA_2$s, like Asp49 secretory phospholipase A_2 from the snake venom of *Agkistrodon piscivorus piscivorus*,[39] can also degrade zwitterionic lipids.[23] This has been explained by the presence of one or more aromatic residues located on the protein binding surface that penetrate the interfacial membrane region, thereby enhancing the binding affinity to zwitterionic membrane surfaces.[40] Other examples include the human secretory phospholipase A_2 type V and X.[41] Clearly, enzyme adsorption of several $sPLA_2$ species are driven by the interplay between the $sPLA_2$ binding surface and lipid interface properties.[38,40,42,43] As shown in Figure 1, phospholipase A_2-IIA has a more positively charged binding surface than snake venom $sPLA_2$ and thereby prefers negatively charged membrane surfaces.[35,44]

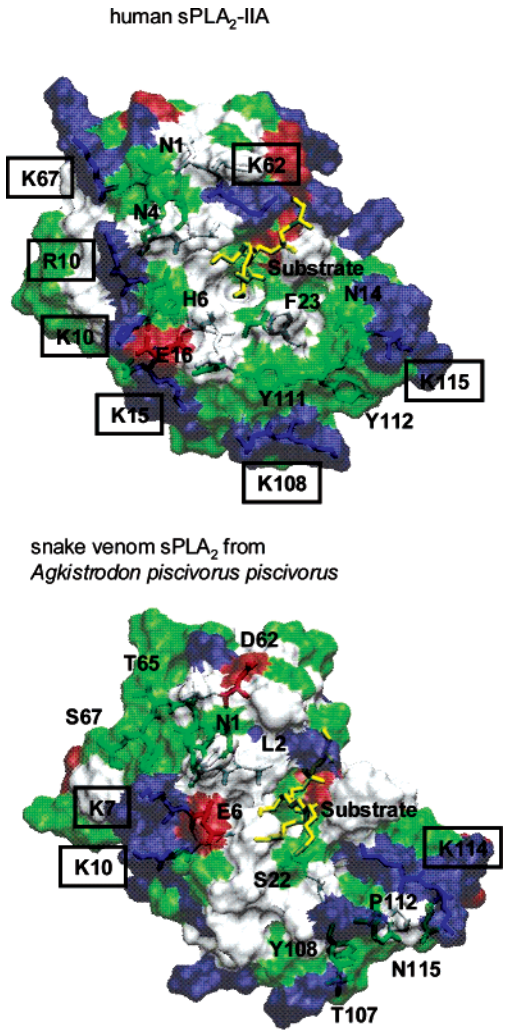

Figure 1. View onto the binding surface (i-face) of human $sPLA_2$-IIA (top) and snake (*Agkistrodon piscivorus piscivorus*) venom $sPLA_2$ (bottom). Coloring of the surface corresponds to the properties of the residues: positively charged (blue), negatively charged (red), polar (green), and aromatic/hydrophobic (gray). Residues that are drawn in stick modus have the right orientation such that they might be involved in contact with the membrane surface.[24,38,40,86] The substrate (**1R**) is shown in stick modus and colored yellow.

Increasing attention has been given to the human secretory phospholipase A_2 type IIA ($sPLA_2$-IIA), a calcium-dependent, ~14 kDa, disulfide-rich enzyme, since it has been implicated in a large variety of physiological processes.[45] $sPLA_2$-IIA is highly expressed in inflammatory tissues, where it hydrolyzes phospholipids to release arachidonic acid that further downstream in the signaling cascade is processed by cyclooxygenases or lipoxygenase to form proinflammatory lipid mediators known as eicosanoids.[32,46,47] $sPLA_2$ has also been shown to be up-

(18) White, S. P.; Scott, D. L.; Otwinowski, Z.; Gelb, M. H.; Sigler, P. B. *Science* **1990,** *250*, 1560−1563.
(19) Scott, D. L.; Otwinowski, Z.; Gelb, M. H.; Sigler, P. B. *Science* **1990**, *250*, 1563−1566.
(20) Kudo, I.; Murakami, M. *Prostaglandins Other Lipid Mediators* **2002**, *68−69*, 3−58.
(21) Dennis, E. A. *J. Biol. Chem.* **1994**, *269*, 13057−13060.
(22) Hønger, T.; Jørgensen, K.; Biltonen, R. L.; Mouritsen, O. G. *Biochemistry* **1996**, *35*, 9003−9006.
(23) Leidy, C.; Linderoth, L.; Andresen, T. L.; Mouritsen, O. G.; Jørgensen, K.; Peters, G. H. *Biophys. J.* **2006**, *90*, 3165−3175.
(24) Mouritsen, O. G.; Andresen, T. L.; Halperin, A.; Hansen, P. L.; Jakobsen, A. F.; Jensen, U. B.; Jensen, M. Ø.; Jørgensen, K.; Kaasgaard, T.; Leidy, C.; Simonsen, A. C.; Peters, G. H.; Weiss, M. *J. Phys. Condens. Matter* **2006**, *18*, 1−12.
(25) Peters, G. H.; Dahmen-Levison, U.; de Meijere, K.; Brezesinski, G.; Toxvaerd, S.; Svendsen, A.; Kinnunen, P. K. J. *Langmuir* **2000**, *16*, 2779−2788.
(26) Carriere, F.; Withers-Martinez, C.; van Tilberugh, H.; Roussel, A.; Cambillau, C.; Verger, R. *Biochim. Biophys. Acta* **1998**, *1376*, 417−432.
(27) Jain, M. K.; Berg, O. G. *Biochim. Biochim. Acta* **1989**, *1002*, 127−156.
(28) Mouritsen, O. G.; Jørgensen, K. *Pharm. Res.* **1998**, *15*, 1507−1519.
(29) Huhtinen, H. T.; Grönroos, J. O.; Grönroos, J. M.; Uksila, J.; Gelb, M. H.; Nevalainen, J.; Laine, V. J. O. *Acta Pathol. Microbiol. Immunol. Scand.* **2006**, *114*, 127−130.
(30) Qu, X. D.; Lehrer, R. I. *Infect. Immun.* **1998**, *66*, 2791−2797.
(31) Bezzine, S.; Koduri, A.; Valentin, E.; Murakami, M.; Kudo, I.; Ghomashchi, F.; Sadilek, M.; Lambeau, G.; Gelb, M. H. *J. Biol. Chem.* **2000**, *275*, 3179−3191.
(32) Murakami, M.; Koduri, R. S.; Enomoto, A.; Shimbara, S.; Seki, M.; Yoshihara, K.; Singer, A.; Valentin, E.; Ghomashchi, F.; Lambeau, G.; Gelb, M. H.; Kudo, I. *J. Biol. Chem.* **2001**, *276*, 10083−10096.
(33) Enomoto, A.; Murakami, A.; Valentin, E.; Lambeau, G.; Gelb, M. H.; Kudo, I. *J. Immunol.* **2000**, *165*, 4007−4014.
(34) Buckland, A. G.; Heeley, E. L.; Wilton, D. C. *Biochim. Biochim. Acta* **2000**, *1484*, 195−206.
(35) Bezzine, S.; Bollinger, J. G.; Singer, A. G.; Veatch, S. L.; Keller, S. L.; Gelb, M. H. *J. Biol. Chem.* **2002**, *277*, 48523−48534.
(36) Bayburt, T.; Yu, B.-Z.; Lin, H.-K.; Browning, J.; Jain, M. K.; Gelb, M. H. *Biochemistry* **1993**, *32*, 573−582.
(37) Kinkaid, A. R.; Wilton, D. C. *Biochem. J.* **1995**, *308*, 507−512.
(38) Scott, D. L.; Mandel, A. M.; Sigler, P. B.; Honig, B. *Biophys. J.* **1994**, *67*, 493−504.
(39) Han, S. K.; Yoon, E. T.; Scott, D. L.; Sigler, P. B.; Cho, W. *J. Biol. Chem.* **1997**, *272*, 3573−3582.
(40) Gelb, M. H.; Cho, W.; Wilton, D. C. *Curr. Opin. Struct. Biol.* **1999**, *9*, 428−432.
(41) Murakami, M.; Kudo, I. *J. Biochem.* **2002**, *131*, 285−292.
(42) Lin, Y.; Nielsen, R.; Murray, D.; Hubbell, W. L.; Mailer, C.; Robinson, B. H.; Gelb, M. H. *Science* **1998**, *279*, 1925−1929.
(43) Ball, A.; Nielsen, R.; Gelb, M. H.; Robinson, B. H. *Proc. Natl. Acad. Sci. U.S.A.* **1999**, *96*, 6637−6642.
(44) Canaan, S.; Nielsen, R.; Ghomashchi, F.; Robinson, B. H.; Gelb, M. H. *J. Biol. Chem.* **2002**, *277*, 30984−30990.
(45) Fuentes, L.; Hernandez, M.; Nieto, M. L.; Crespo, M. S. *FEBS Lett.* **2002**, *531*, 7−11.

regulated in a variety of cancer types[48,49] including prostate,[50,51] colon,[52,53] breast,[54] and pancreatic cancer.[55,56] It has been suggested that the $sPLA_2$-IIA overexpression in cancerous tissue may be triggered by the carcinoma cells and hepatocytes and/or inflammatory cells (e.g., macrophages) by stimulation of inflammatory cytokines.[48,57] The observation that many tumors have elevated $sPLA_2$ levels highlights that $sPLA_2$ plays a central role in tumor development and demonstrates that $sPLA_2$ is a potential target for therapeutic intervention.[58,59] Indeed, it has been demonstrated that elevated concentrations of $sPLA_2$ in cancer cells can be used as a suitable tumor-specific triggering mechanism for liposome-based anticancer drug carriers.[59−62] Liposomes comprised of natural phospholipids or anticancer lipid-based prodrugs are hydrolyzed by $sPLA_2$ resulting in a controlled release of the cytotoxic drugs into the tumor tissue.[62,63] This approach results in increased circulation life time, enhanced deposition to the malignant tissue, and protection from the drug metabolic degradation.[64] The usage of natural lipids has a further advantage in that these systems are biodegradable, are weakly immunogenic, possess limited intrinsic toxicity, and produce no antigenic or pyrogenic reactions.[65,66] These liposome-based drug carries can be optimized with respect to, e.g., circulation lifetime, stability ("leakage" of drugs), or hydrolysis by $sPLA_2$ by changing lipid composition, modifying their surface characteristics (e.g., polymer-grafted liposomes), or using unnatural phospholipid analogues degradable by $sPLA_2$.[28,63,67]

We have previously shown, in a rapid report,[67] that unnatural phospholipid analogues with the head group in the 2-position not only form stable liposomes with intriguing phase behavior but also are efficiently degraded by $sPLA_2$. Although $sPLA_2$ shows lower activity toward the unnatural phospholipid analogues, it is intriguing that $sPLA_2$ can also hydrolyze lipids with head groups located in the 2-position. To provide further insight on a molecular level and to explain the altered $sPLA_2$ activity, we report here molecular dynamics simulations of six different $sPLA_2$−phospholipid substrate complexes (Figure 2) and compare the results with experiments. The simulations revealed that the unnatural lipids are positioned in the $sPLA_2$ binding pocket in such a way that the lipids interfere with an incoming water molecule that participates in the hydrolysis. The probability of a water molecule reaching the correct position such that hydrolysis can occur is reduced for the unnatural lipids. This in part could explain the experimentally observed reduced $sPLA_2$ activity profile toward the unnatural phospholipid analogues.

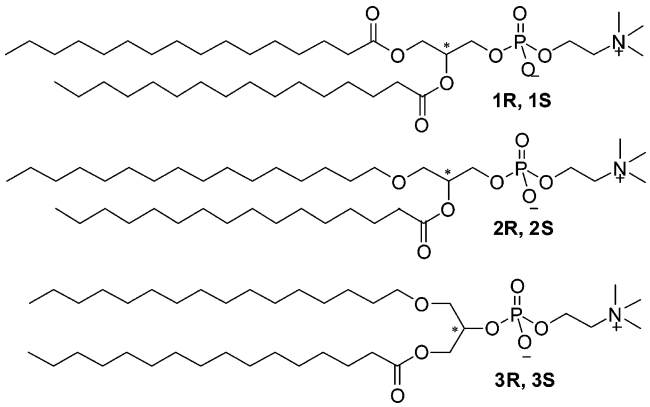

Figure 2. Chemical structures of the three enatiomeric pairs (six phospholipids) that have been investigated by molecular dynamics simulations. (**1R**) (*R*)-1,2-dipalmitoyl-glycero-3-phosphocholine, (**1S**) (*S*)-1,2-dipalmitoyl-glycero-3-phosphocholine, (**2R**) (*R*)-1-*O*-hexadecyl-2-palmitoyl-*sn*-glycero-3-phoshocholine, (**2S**) (*S*)-1-*O*-hexadecyl-2-palmitoyl-*sn*-glycero-3-phoshocholine, (**3S**) (*S*)-1-*O*-hexadecyl-3-palmitoyl-glycero-2-phosphocholine, and (**3R**) (*R*)-1-*O*-hexadecyl-3-palmitoyl-glycero-2-phosphocholine. The compounds with the correct stereochemistry for $sPLA_2$ hydrolysis, **1R**, **2R**, and **3S** have been synthesized, and liposomes constituted of these phospholipids have been investigated experimentally.

Experimental Section

Materials and Liposome Preparation. 1,2-Dipalmitoyl-*sn*-glycero-3-phosphocholine (DPPC, **1R**) was purchased from Avanti Polar Lipids, Birmingham, AL. All other lipids were synthesized. All other chemicals were purchased from Sigma-Aldrich. One-component multilamellar liposomes were prepared by hydrating the lipids in a Hepes buffer solution for 1 h 10−15 °C above the main phase transition of the multilamellar liposomes. The lipid suspension was vortexed every 15 min. Unilamellar liposomes of narrow size distribution were made by extrusion of the multilamellar liposome suspension 10 times through two stacked 100 nm polycarbonate filters. The Hepes buffer used was composed of the following: 0.15 M KCl, 1 mM NaN_3, 0.03 mM $CaCl_2$, 0.01 mM EDTA, 0.01 M Hepes (pH = 7.5).

Differential Scanning Calorimetry. Differential scanning calorimetry (DSC) of 5 mM multilamellar liposomes was performed using a Microcal MC-2 (Northhampton, MA) ultrasensitive power-compensating scanning calorimeter equipped with a nanovoltmeter. The scans were performed in the upscan mode at a scan rate of 20 °C/h. An appropriate baseline has been subtracted from the calorimetric curves.

Phospholipase A_2 Activity Measurements. The employed $sPLA_2$ (*Agkistrodon piscivoros piscivoros*) was isolated and purified from snake venom.[68] This enzyme is structurally similar to mammalian $sPLA_2$, indicating a similar catalytic hydrolysis mechanism for phos-

(46) Kim, Y. J.; Kim, K. P.; Han, S. K.; Munoz, N. M.; Zhu, X.; Sano, H.; Leff, A. R.; Cho, W. *Biol. Chem.* **2002**, *277*, 36479−36488.
(47) Glomset, J. A. *Curr. Opin. Struct. Biol.* **1999**, *9*, 425−427.
(48) Abe, T.; Sakamoto, K.; Kamohara, H.; Hirano, Y.; Kuwahara, N.; Ogawa, M. *Intern. Congress Series* **2003**, *1255*, 351−360.
(49) Abe, T.; Sakamoto, K.; Kamohara, H.; Hirano, Y.; Kuwahara, N.; Ogawa, M. *Int. J. Cancer* **1997**, *74*, 245−250.
(50) Sved, P.; Scott, K. F.; McLeod, D.; King, N. J. C.; Singh, J.; Tsatralis, T.; Nikolov, B.; Boulas, J.; Nallan, L.; Gelb, M. H.; Sajinovic, M.; Graham, G. G.; Russell, P. J.; Dong, Q. *Cancer Res.* **2004**, *64*, 6934−6940.
(51) Jiang, J.; Neubauer, B. L.; Graff, J. R.; Chedid, M.; Thomas, J. E.; Roehm, N. W.; Zhang, S.; Eckert, G. J.; Koch, M. O.; Eble, J. N.; Cheng, L. *Am. J. Pathology* **2002,** *160*, 667−671.
(52) Ilsley, J. N. M.; Nakanishi, M.; Flynn, C.; Belinsky, G. S.; De, Guise, S.; Adib, J. N.; Dobrowsky, R. T.; Bonventre, J. V.; Rosenberg, D. W. *Cancer Res.* **2005**, *65*, 2636−2643.
(53) Edhemovic, I.; Snoj, M.; Kljun, A.; Golouh, R. *EJSO* **2001**, *27*, 545−548.
(54) Yamashita, S.; Yamashita, J.; Ogawa, M. *Br. J. Cancer* **1994**, *69*, 1166−1170.
(55) Kiyohara, H.; Egami, H.; Kurizaki, T.; Murata, K.; Ohmachi, H.; Akagi, J.; Ohshima, S.; Yamamoto, S.; Shibata, Y.; Ogawa, M. *Intern. Congress Series* **2003**, *1255*, 375−379.
(56) Hanada, K.; Kinoshita, E.; Itoh, M.; Hirata, M.; Kajiyama, G.; Sugiyama, M. *FEBS Lett.* **1995**, *373*, 85−87.
(57) Yamashita, S.; Ogawa, M.; Abe, T.; Yamashita, J.; Sakamoto, K.; Niwa, H.; Yamamura, K. *Biochem. Biophys. Res. Commun.* **1994**, *198*, 878−884.
(58) Laye, J.; Gill, J. H. *Drug Discovery Today* **2003**, *8*, 710−716.
(59) Andresen, T. L.; Jensen, S. S.; Jørgensen, K. *Prog. Lipid Res.* **2005**, *44*, 68−97.
(60) Andresen, T. L.; Jensen, S. S.; Kaasgaard, T.; Jørgensen, K. *Curr. Drug Delivery* **2005**, *2*, 353−362.
(61) Jørgensen, K.; Davidsen, J.; Mouritsen, O. G. *FEBS Lett.* **2002**, *531*, 23−27.
(62) Andresen, T. L.; Davidsen, J.; Begtrup, M.; Mouritsen, O. G.; Jørgensen, K. *J. Med. Chem.* **2004**, *47*, 1694−1703.
(63) Goyal, P.; Goyal, K.; Kumar, S. G. V.; Singh, A.; Katare, O. P.; Mishra, D. N. *Acta Pharm.* **2005**, *55*, 1−25.
(64) Jensen, S. S.; Andresen, T. L.; Davidsen, J.; Høyrup, P.; Shnyder, S. D.; Bibby, M. C.; Gill, J. H.; Jørgensen, K. *Mol. Cancer Ther.* **2004**, *3*, 1451−1458.
(65) Van Rooijen, N.; van Nieuwmegen, R. *Immunol. Commun.* **1980**, *9*, 243−256.
(66) Campbell, P. I. *Cytobios* **1983**, *37*, 21−26.
(67) Andresen, T. L.; Jørgensen, K. *Biochim. Biophys. Acta* **2005**, *1669*, 1−7.

pholipid substrates.[69] Assay conditions for the $sPLA_2$ lag-time measurements were 0.15 mM unilamellar liposomes in a Hepes buffer (150 nM $sPLA_2$, 0.15 M KCl, 1 mM NaN_3, 0.03 mM $CaCl_2$, 0.01 mM EDTA, and 0.01 M Hepes (pH = 7.5)). The catalytic reaction was initiated by adding 8.9 μL of a 42 μM $sPLA_2$ stock solution to 2.5 mL of a thermostated liposome suspension equilibrated 20 min prior to addition of the enzyme. The time elapsed between addition of $sPLA_2$ and a sudden increase in the intrinsic fluorescence emission from $sPLA_2$ (tryptophan emission), due to a burst in the $sPLA_2$ activity, is defined as the characteristic lag time of the enzyme. The emission takes place at 340 nm after excitation at 285 nm. The total amount of hydrolyzed lipid 1000 s after the $sPLA_2$ burst was determined by HPLC.

HPLC Quantification. HPLC analysis was performed using a 5 μL diol column, a mobile phase composed of $CHCl_3$/MeOH/H_2O (730:230:25, v/v), and an evaporative light scattering detector. Sample (100 μL) was withdrawn from a 0.15 mM liposome suspension, which was rapidly mixed with 1 mL of $CHCl_3$/methanol/acetic acid (2:4:1) in order to quench the enzymatic reaction. The solution was washed with 1 mL of water, and 20 μL of the organic phase were used for HPLC.

Synthesis of (*R*)-1-*O*-Hexadecyl-*sn*-glycero-3-phosphocholine (2R) from (*R*)-*O*-Benzyl Glycidol (4R). Carried out as earlier described by Andresen and co-workers.[62]

Synthesis of (*S*)-1-*O*-Hexadecyl-3-*O*-benzyl-glycerol (6). To a flame-dried flask containing washed NaH (0.23 g, 9.6 mmol) under N_2 at 0 °C cetylalcohol (1.94 g, 8.02 mmol) in dry THF (20 mL) was added. The NaH was washed by a continuous extraction of the NaH dispersion (60% mineral oil) with dry hexane. The reaction was heated to 80 °C for 1 h. (*S*)-*O*-Benzyl glycidol (**4S**) (1.05 g, 6.1 mmol) was added followed by DMF (10 mL). The reaction was stirred overnight at 80 °C. The reaction was cooled to room temperature and stirred 20 min after the addition of water (2 mL). Removal of solvent in vacuo gave a brown residue, which was redissolved in ether (40 mL), washed with brine (5 × 10 mL), and dried over Na_2SO_4. Purification by flash chromatography (CH_2Cl_2/ether 100:1) gave 1.86 g (71%) of **6**. R_f = 0.11 (CH_2Cl_2/ether 100:1). ^{1}H NMR (300 MHz, $CDCl_3$): δ 7.32 (m, 5H), 4.56 (s, 2H), 4.00 (m, 1H), 3.60−3.30 (m, 6H), 1.59 (m, 2H), 1.26 (br.s, 26H) 0.88 (t, 3H). ^{13}C NMR (75 MHz, $CDCl_3$): δ 138.3, 128.6, 127.9, 73.6, 72.1, 71.9, 71.7, 69.7, 32.2, 30.0, 29.9, 29.9, 29.9, 29.8, 29.7, 26.4, 23.0, 14.4.

Synthesis of (*S*)-1-*O*-Hexadecyl-3-*O*-benzyl-glycero-2-phosphocholine (7). To a solution of $POCl_3$ (79.8 μL, 0.856 mmol) in dry CH_2Cl_2 (0.5 mL) under N_2 at 0 °C a solution of **6** (272.2 mg, 0.679 mmol) and Et_3N (0.13 mL, 0.910 mmol) in CH_2Cl_2 (2 mL) was added dropwise over 15 min. The reaction mixture was stirred for 1 h under N_2 at room temperature, after which pyridine (0.44 mL, 5.43 mmol) and choline tosylate (374 mg, 1.36 mmol) were added at 0 °C. After 2 h, the orange reaction mixture was allowed to warm to room temperature and was left stirring overnight. After 24 h of stirring, TLC (CH_2Cl_2/MeOH/H_2O 65:25:4) indicated that the reaction had gone to completion. Water (0.2 mL) was added, and the reaction mixture was stirred for 1 h and concentrated to a white solid by azeotropic distillation with toluene. The residue was dissolved in THF/H_2O 9:1 and slowly passed through an MB-3 column (2 cm), and the solvent was removed by azeotropic distillation with ethanol and toluene in vacuo. The crude product was purified by column chromatography (CH_2Cl_2/MeOH/H_2O 65:25:1) giving **7** in 253 mg (65%). R_f = 0.17 (CH_2Cl_2/MeOH/H_2O 65:25:1). ^{1}H NMR (300 MHz, $CDCl_3$): δ 7.32 (m, 5H), 4.54 (s, 2H), 4.40 (m, 1H), 4.20 (m, 2H), 3.78−3.45 (m, 6H), 3.40 (t, J = 6.1 Hz, 2H), 3.08 (s, 9H), 1.59 (m, 2H), 1.26 (br.s, 26H), 0.89 (t, 3H). ^{13}C NMR (75 MHz, $CDCl_3$): δ 138.3, 128.6, 127.9, 73.5, 73.2 (d, J = 7.3 Hz), 71.7, 71.6 (d, J = 4.9 Hz), 70.9 (d, J = 4.8 Hz), 66.3 (d, J = 5.3 Hz), 59.2 (d, J = 4.8 Hz), 54.4, 32.1, 29.9, 29.8, 29.6, 29.4, 26.3, 25.2, 22.9, 14.3.

Synthesis of (*R*)-1-*O*-Hexadecyl-3-lyso-glycero-2-phosphocholine (8). To a solution of **7** (253 mg, 0.442 mmol) in EtOAc/MeOH (20 mL, 1:1) under N_2 at room temperature Pd/C 10% (33 mg) was added. The reaction mixture was placed under H_2 with vigorous stirring for 1.5 h, after which TLC (CH_2Cl_2/MeOH/H_2O 65:25:4) showed no remaining starting material. The solution was filtered through a glass filter, which was washed successively with CH_2Cl_2. Concentrating in vacuo gave 213 mg (quantitative) of **8** as a white solid, which was dried at 0.1 mmHg for 1 h and used without further purification in the next step. R_f = 0.13 (CH_2Cl_2/MeOH/H_2O 65:25:4). ^{1}H NMR (300 MHz, $CDCl_3$/CD_3OD 9:1): δ 4.20−4.10 (m, 3H), 3.65−3.25 (m, 8H), 3.20−3.08 (m, 9H), 1.59 (m, 2H), 1.26 (br.s, 26H), 0.88 (t, 3H). ^{13}C NMR (75 MHz, $CDCl_3$/CD_3OD 9:1): δ 76.1 (d, J = 7.4 Hz), 71.8, 71.1 (d, J = 5.1 Hz), 66.4 (d, J = 6.1 Hz), 63.9 (d, J = 4.8 Hz), 59.5 (d, J = 4.7 Hz), 54.4, 32.1, 29.9, 29.8, 29.6, 29.4, 26.3, 25.2, 22.9, 14.3.

Synthesis of (*S*)-1-*O*-Hexadecyl-3-palmitoyl-glycero-2-phosphocholine (3S). 8 (236 mg, 0.49 mmol) was dissolved in dry CH_2Cl_2 (25 mL) to which Et_3N (0.17 mL, 1.22 mmol), DMAP (24 mg, 0.20 mmol), and palmitoyl chloride (0.37 mL, 1.22 mmol) were added. The yellow reaction mixture was stirred overnight at room temperature, after which TLC (CH_2Cl_2/MeOH/H_2O 65:25:4) indicated that the reaction had gone to completion. The reaction mixture was concentrated and purified by flash chromatogaphy (CH_2Cl_2/MeOH/H_2O 65:25:1 → CH_2Cl_2/MeOH/H_2O 65:25:4) to give 294 mg (83%) of **3S**. R_f = 0.28 (CH_2Cl_2/MeOH/H_2O 65:25:4). ^{1}H NMR (300 MHz, $CDCl_3$): δ 4.45−4.18 (m, 5H), 3.80 (m, 2H) 3.57 (m, 2H), 3.45−3.23 (m, 11H), 2.30 (t, J = 6.7 Hz, 2H), 1.59 (m, 2H), 1.51 (m, 2H), 1.26 (br.s, 50H), 0.88 (t, 6H). ^{13}C NMR (75 MHz, $CDCl_3$): δ 173.8, 76.9 (d), 71.8, 70.4 (d), 66.2 (d), 63.8 (d), 59.4 (d), 54.5, 35.5, 32.1, 29.9, 29.8, 29.6, 29.4, 26.3, 25.2, 22.9, 14.3.

Molecular Dynamics Simulations. The crystal structures of (i) European Honeybee (*Apis Mellifera*)-venom phospholipase A_2 complexed with the transition-state analogue, 1-*O*-octyl-2-heptylphosphonyl-*sn*-glycero-3-phosphoethanolamine (diC_8(2Ph)PE), resolved to 2.0 Å[19] and (ii) Human $sPLA_2$−IIA complexed with 6-phenyl-4(*R*)-(7-phenyl-heptanoylamino)-hexanoic acid resolved to 2.1 Å[70] were obtained from the Protein Data Bank[71] (entry codes: 1poc and 1kqu, respectively). The initial modeling step involved placing diC_8(2Ph)PE into the binding cleft of $sPLA_2$-IIA, which was done by (i) deleting the inhibitor in 1kqu (keeping calcium ions and water molecules in the structure), (ii) deleting calcium ions and water molecules in 1poc, (iii) aligning 1poc with 1kqu, and (iii) finally deleting the bee-venom phospholipase A_2 structure. The structures of the six phospholipids (Figure 1) were built from diC_8(2Ph)PE using SPARTAN version 1.0.2 (Wavefunction Inc., Irvine, California). Missing distance, angle, and torsion parameters were obtained from the CHARMM27 parameter set describing similar atom types. The structures were solvated using the program SOLVATE.[72] To neutralize the systems, 18 water molecules were randomly replaced with chloride ions. The final systems contained ~4900 water molecules, and the simulation cell dimensions were ~53 × 52 × 67 Å^3. For the simulations, the molecular dynamics (MD) program NAMD[73] was used with the Charmm27 all hydrogens parameter set and with the TIP3 water model.[74] Each complex was simulated at least three times (Table 1) starting from different initial conditions, which were obtained by varying the number of steps used in energy minimization of the systems.

(68) Maraganore, J. M.; Merutka, G.; Cho, W.; Welches, W.; Kezdy, F. J.; Heinrikson, R. L. *J. Biol. Chem.* **1984**, *259*, 13839−13843.
(69) Vance, D. E.; Vance, J. E. *Biochemistry of Lipids, Lipoproteins and Membranes*; Elsevier: Amsterdam, 1991.
(70) Hansford, K. A.; Reid, R. C.; Clark, C. I.; Tyndall, J. D. A.; Whitehouse, M. W.; Guthrie, T.; McGeary, R. P.; Schafer, K.; Martin, J. L.; Fairlie, D. P. *ChemBioChem* **2003**, *4*, 181−185.
(71) Bernstein, F. C.; Koetzle, T. F.; Williams, G. J.; Meyer, E. E.; Brice, M. D.; Rodgers, J. R.; Kennard, O.; Shimanouchi, T.; Tasumi, M. *J. Mol. Biol.* **1977**, *112*, 535−542.
(72) Grubmüller, H. Solvate: a program to create atomic solvent models. Electronic publication: http://www.mpibpc.gwdg.de/abteilungen/071/solvate/docu.html.
(73) Kale, L.; Skeel, R.; Bhandarkar, M.; Brunner, R.; Gursoy, A.; Krawetz, N.; Phillips, J.; Shinozaki, A.; Varadarajan, K.; Schulten, K. *J. Comput. Phys.* **1999**, *151*, 283−312.
(74) Jorgensen, W. L.; Chandrasekhar, J.; Medura, J. D.; Impey, R. W.; Klein, M. L. *J. Chem. Phys.* **1983**, *79*, 926−935.

Table 1. Summary of the Simulations Carried Out[a]

name	short name[b]	number of simulations	length of simulations (ns)	root-mean-square displacement mean ± SD[c] (Å)
(*R*)-1,2-dipalmitoyl-glycero-3-phosphocholine	**1R**	6	each 10	1.3 ± 0.1
(*S*)-1,2-dipalmitoyl-glycero-3-phosphocholine	**1S**	4	each 10	1.5 ± 0.1
(*R*)-1-*O*-hexadecyl-2-palmitoyl-*sn*-glycero-3-phoshocholine	**2R**	3	each 10	1.4 ± 0.1
(*S*)-1-*O*-hexadecyl-2-palmitoyl-*sn*-glycero-3-phoshocholine	**2S**	3	each 10	1.5 ± 0.1
(*R*)-1-*O*-hexadecyl-3-palmitoyl-glycero-2-phosphocholine	**3R**	3	each 10	1.4 ± 0.1
(*S*)-1-*O*-hexadecyl-3-palmitoyl-glycero-2-phosphocholine	**3S**	3	each 10	1.3 ± 0.1

[a] The last column lists the average root-mean-square displacement of Cα atoms with respect to the protein structure obtained after minimization. Averages and standard deviations (SDs) are based on a series of simulations of a particular complex. [b] Abbreviation used in the text. [c] SD = standard deviation calculated as follows: $SD = \sqrt{\sum_{i=1}^{N}(x_i-\bar{x})^2/(N-1)}$.

Scheme 1

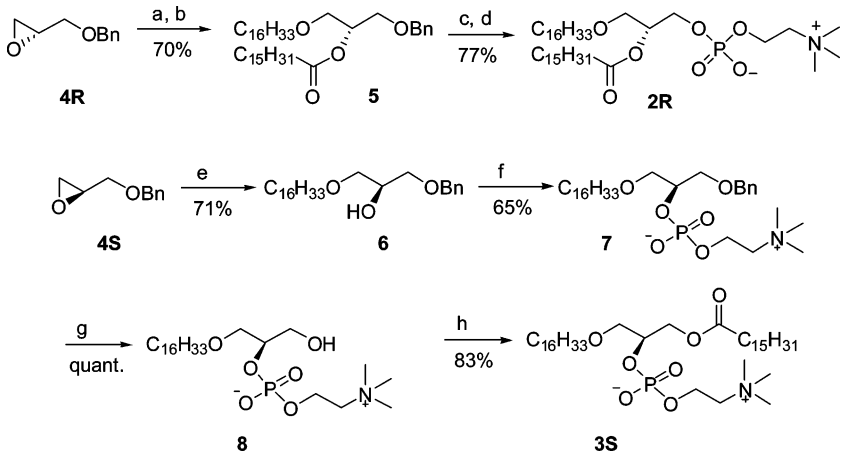

The first energy minimization of the systems involved 250 steps. For each subsequent simulation of a certain complex, the number of steps for energy minimization was increased by 250 steps; i.e., 250, 500, and 750 steps were used for simulations of a complex that was repeated three times. The minimization procedure was followed by 100 ps of heating of the systems to $T = 300$ K. The simulations were carried out for 10 ns at constant number of atoms, pressure, and temperature (*NPT* ensemble). Periodic boundary conditions were applied in *x*, *y*, and *z*-directions. A time step of 1 fs was used throughout all simulations. An isotropic constant ambient pressure of 1 atm was imposed using the Langevin piston method[75] with a damping coefficient of 5 ps^{-1}, a piston period of 200 fs, and a decay of 500 fs. The Particle Mesh Ewald method was used for computation of the electrostatic forces.[76,77] The grid spacing applied was approximately 1.0 Å, and a fourth order spline was used for the interpolation. The long-range part of the electrostatic forces was evaluated every fourth femtosecond. The van der Waals interactions were cut off at 12 Å using a switching function starting at 10 Å. The analyses of the trajectories were performed using the graphical program Visualization Molecular Dynamics (VMD).[78]

Results and Discussion

We have demonstrated earlier that the presence of phosphoglycerol (PG) in phosphocholine (PC) membranes enhances $sPLA_2$-IIA activity, and at the same time, both lipid species are hydrolyzed by $sPLA_2$-IIA.[23] This observation supports the view that in the case of snake venom $sPLA_2$ and human $sPLA_2$-IIA, the activity of these enzymes is determined mainly by the physical properties of the membrane surface.[79,80] Our primary aim in the present study is to investigate by molecular dynamics simulations the binding mode of phospholipid analogues and to understand in molecular detail the basis for the modified $sPLA_2$ activity toward phospholipid analogues with head groups located in the 2-position when compared to its natural substrate. As summarized in Table 1, we have studied six different phospholipids (Figure 2) in complex with human $sPLA_2$-IIA.[70] **1R** is the natural substrate for $sPLA_2$. **1S** has been included as a reference, since, due to the stereospecific enzyme reaction, this phospholipid should not be hydrolyzed by $sPLA_2$. **2R** and **2S** contain an ether bond in the 1-position of the glycerol backbone instead of the natural ester group. This replacement was done for practical purposes, to avoid uncontrolled hydrolysis by the enzyme when moving the head group to the 2-position. **3R** and **3S** are the two phospholipid enantiomers with the head groups located at the 2-position of the glycerol backbone. Simulation of each enzyme-phospholipid complex was repeated at least three times to increase the statistical significance of our

(75) Feller, S. E.; Zhang, Y.; Pastor, R. W.; Brooks, B. R. *J. Chem. Phys.* **1995**, *103*, 4613−4621.
(76) Darden, T.; York, D.; Pedersen, L. *J. Chem. Phys.* **1993**, *98*, 10089−10092.
(77) Essmann, U.; Perera, L.; Berkowitz, M. L.; Darden, T.; Lee, H.; Pedersen, L. G. *J. Chem. Phys.* **1995**, *103*, 8577−8593.
(78) Humphrey, W.; Dalke, A.; Schulten, K. *J. Mol. Graph.* **1996**, *14*, 33−38.
(79) Pan, Y. H.; Yu, B.-Z.; Berg, O. G.; Jain, M. K.; Bahnson, B. J. *Biochemistry* **2002**, *41*, 14790−14800.
(80) Bahnson, B. J. *Arch. Biochem. Biophys.* **2005**, *433*, 96−106.

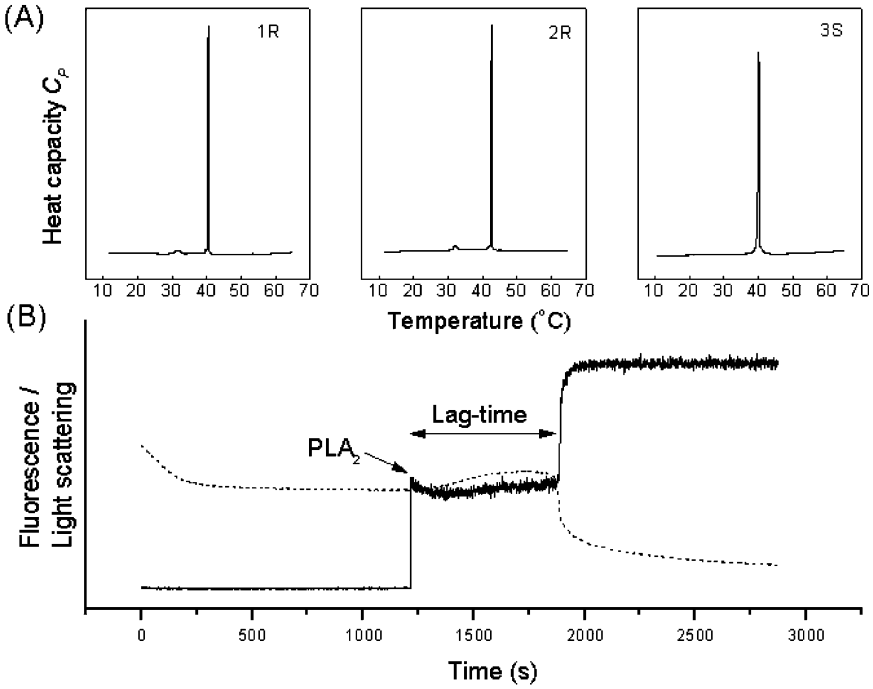

Figure 3. (A) Differential scanning heat capacity curves obtained at a scan rate of 20 °C/h for 5 mM multilammelar liposomes composed of **1R**, **2R**, and **3S**. (B) Characteristic $sPLA_2$ (*Agkistrodon piscivorus piscivorus*) activity time course profiles toward unilamellar liposomes. The $sPLA_2$ activity is monitored by intrinsic fluorescence (solid line) from the enzyme and by 90° light scattering (dashed line) from the lipid suspension.

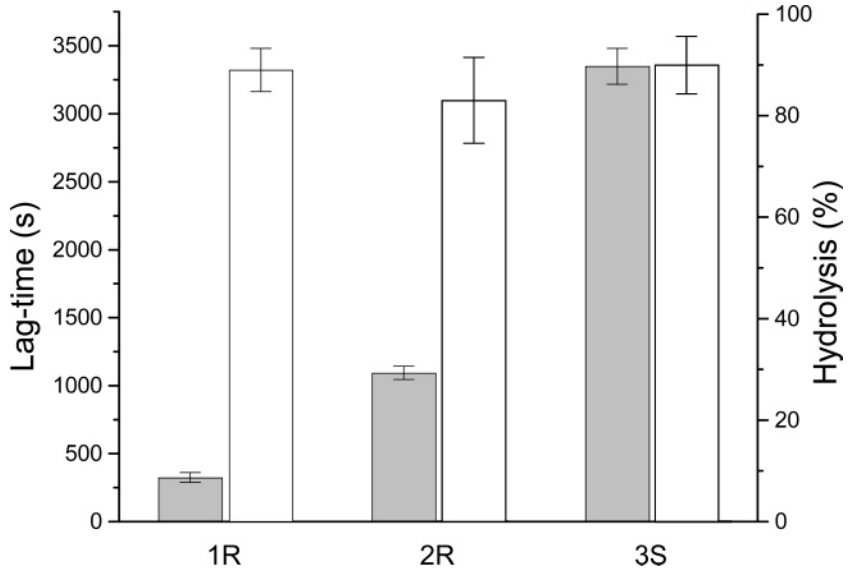

Figure 4. Secretory PLA_2 lag times for **1R**, **2R**, and **3S** obtained at the main phase transition temperature (gray bars). Total hydrolysis of the three phospholipids measured by HPLC 1000 s after the burst has occurred (white bars).

results. As outlined in the Experimental Section, each simulation for a particular $sPLA_2$−phospholipid complex was started from different initial conditions by varying the steps used for the initially performed energy minimization.

Synthesis and Biophysical Investigations. To compare the results from our molecular dynamics simulations with experiments, we have synthesized **2R** and **3S** (Figure 2) that both, together with the commercially available **1R** (DPPC), have the right stereochemistry for $sPLA_2$ hydrolysis. **2R** was synthesized from (*R*)-*O*-benzyl glycidol (Scheme 1) in four steps as described in detail by our group in an earlier article.[62] **3S** was synthesized starting from (*S*)-*O*-benzyl glycidol (**4S**). The epoxide **4S** was opened regioselectively by reaction with sodium cetyl alkoholate using THF/DMF (2:1) giving **6** in 71% yield. It should be noted that the use of THF afforded considerably reduced dimerization compared to using DMF alone. Phosphorylation using phosphorus oxychloride in DCM gave **7** in 65% yield. Hydrogenation with Pd/C as catalyst followed by acylation using palmitoyl chloride gave the target compound **3S** in 83% yield. One can equally well use palmitic acid and DCC as coupling reagents under standard conditions.

Multilamellar liposomes were prepared from each lipid **1R**, **2R**, and **3S**, and heat capacity (C_p) curves were obtained using differential scanning calorimetry (Figure 3A). The C_p curves show that all three lipids form liposomes with **1R**, **2R**, and **3S** having a main phase transition peak at 40.5, 42.6, and 40.1 °C, respectively, reflecting the gel-to-fluid phase transition. Interestingly, the pretransition that usually characterizes the phase

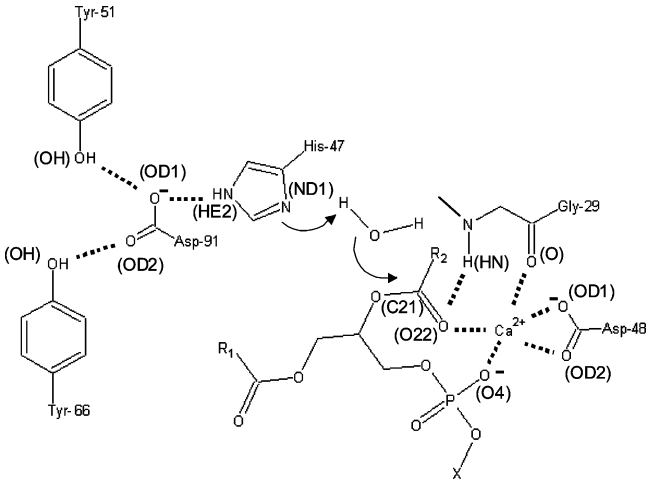

Figure 5. Schematic representation of the catalytic mechanism of $sPLA_2$ and part of the hydrogen-bonding network. Atom types given in parentheses refer to Protein Data Bank nomenclature.

behavior of natural phospholipids,[15,16] such as DPPC (**1R**, seen at 31.9 °C), is abolished for the unnatural phospholipid **3S** with the head group in the 2-position. This may be due to the symmetry in the lipid that is introduced by moving the head group from the 3- to the 2-position.[67] Furthermore, the thermograms revealed that the introduction of an ether bond in the 1-position does not change the phase behavior drastically (Figure 3A).

Unilamelar liposomes for $sPLA_2$ activity measurements were prepared by extrusion through 100 nm polycarbonate filters. A typical $sPLA_2$ (*Agkistrodon piscivorus piscivorus*) fluorescence activity profile can be seen in Figure 3B. After addition of $sPLA_2$, there is a lag time period that reflects a relatively low $sPLA_2$ activity, which suddenly changes in a burst of activity as a consequence of accelerated hydrolysis. The fluorescence is measured as intrinsic fluorescence from the enzyme. Simultaneously with the sudden increase in fluorescence, a decrease in the 90° static light scattering is observed indicating changes in suspension morphology as non-bilayer forming lyso-phospholipids and fatty acids are formed. Figure 4 shows the lag time for lipids **1R**, **2R**, and **3S** at the main phase transition, where the enzyme is known to have the highest activity.[23,62] The natural **1R** (DPPC) has the shortest lag time indicating that this is the best substrate for $sPLA_2$. It is also seen that the introduction of an ether bond in the 1-position (**2R**) results in a longer lag time; however, the change is relatively small. A larger change is observed when moving the phospholipid head group to the 2-position (**3S**). For **3S**, the lag time is increased considerably when compared with the other two phospholipids. Figure 4 also shows the total amount of hydrolysis 1000 s after the accelerated hydrolysis (burst) has occurred. All three phospholipids are hydrolyzed to a high extent after the burst has occurred, and hence, all three lipids are good substrates for $sPLA_2$.

Simulations - Enzyme Stability. The stability of the simulations of the different $sPLA_2$−phospholipid complexes were checked by computing the time evolution of the root mean displacement (rmsd) of the Cα atoms with respect to the protein structure obtained after minimization. A representative time evolution of rmsd calculated from an $sPLA_2$−**1R** simulation is provided as Supporting Information (Figure S1). Means and standard deviations of the rmsd data calculated for the different systems are summarized in Table 1. The relatively low rmsd values reflect the rigid structure of $sPLA_2$-IIA that is caused by eight sulfur bridges. The protein structures complexed with the different phospholipids are stable resulting in an overall rmsd of (1.4 ± 0.1) Å, calculated from the rmsd of each simulation. To further evaluate our simulations, we compared the time-averaged fluctuations of the residues with the B-factor given as part of the X-ray structure,[70] and overall, good agreement was observed between the B-factor and the simulation results (representative results are provided as Supporting Information; Figure S2). In some regions, larger rmsd values are seen in the simulations than in the B-factor. Particularly, protein segments that are located in the vicinity of the substrate (close to the head group and the end of the acyl chains) and in two loop regions are more flexible in the simulations than deduced from the

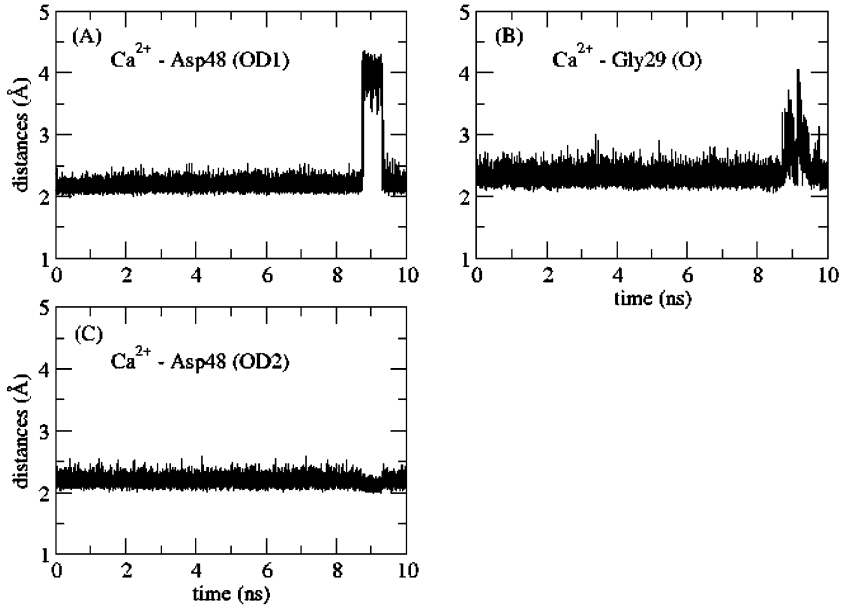

Figure 6. Time evolution of selected distances involving the cofactor calcium. Atom types correspond to the Protein Data Bank nomenclature. The distances were extracted from an $sPLA_2$−**1R** complex simulation and are representative for all simulations.

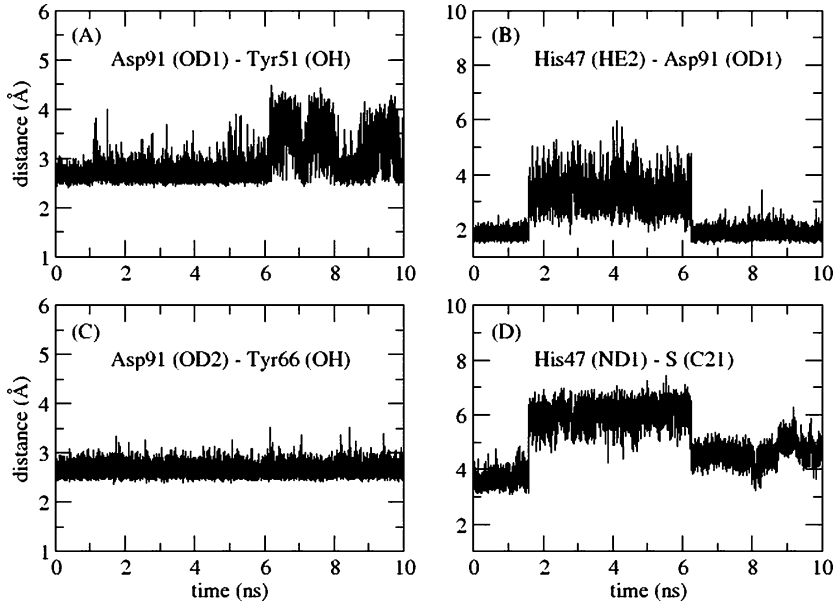

Figure 7. Time evolution of selected distances that involve Asp91 or His47. S and atom types refer to substrate and Protein Data Bank nomenclature, respectively. The distances were extracted from an $sPLA_2$−**1R** simulation and are representative for all simulations.

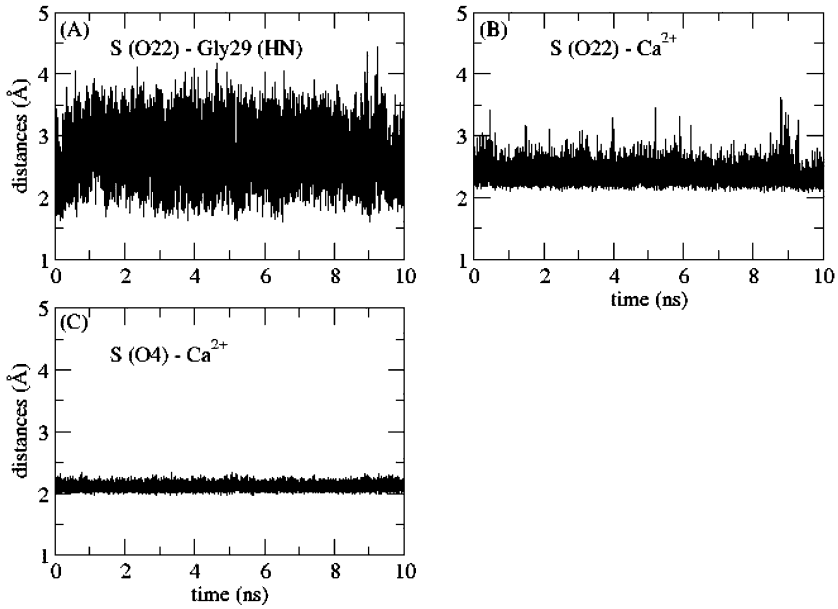

Figure 8. Time evolution of selected distances that involve the substrate (S). See Figure 7 caption for more details.

B-factor. The latter observation is not surprising, since these loop regions are solvent exposed and may be affected by crystal packing.[81] We also calculated the rmsd variation between simulations of a particular complex and between all simulations. We determined an average structure for each simulation using the last 5 ns of the trajectory and calculated consequently the rmsd between the average structures. The rmsd within a series of simulations of a particular complex varies between 0.48 and 0.65 Å yielding (0.57 ± 0.07) Å. The rmsd calculated between average structures of different $sPLA_2$−phospholipid complexes varies between 0.60 and 0.98 Å resulting in (0.72 ± 0.09) Å. Both average rmsd values are the same within the statistical uncertainties indicating that all simulations converge to similar structures.

Simulations - Key Distances. Further structural information was extracted from the simulations by calculating distances between selected atoms (residues). We also calculated the corresponding interaction energies (data not shown), and as expected, there is a direct correlation between calculated interaction energies and monitored distances.[82] In the following, we therefore only report distances. The distances were chosen accordingly to their importance in the calcium-dependent enzymatic reaction.[83] X-ray crystallography revealed that the catalytic device of $sPLA_2$ is essentially characterized by an Asp-His dyad, a calcium-binding site, and a water molecule, which

(81) Peters, G. H.; Bywater, R.P. *J. Mol. Recog.* **2002**, 15 393−403.

(82) Peters, G. H.; Iversen, L. F.; Andersen, H. S.; Møller, N. P. H.; Olsen, O. H. *Biochemistry* **2004**, *43*, 18−28.

(83) Scott, D. L.; White, S.; Otwinowski, Z.; Yuan, W.; Gelb, M. H.; Sigler, P. B. *Science* **1990**, *250*, 1541−1546.

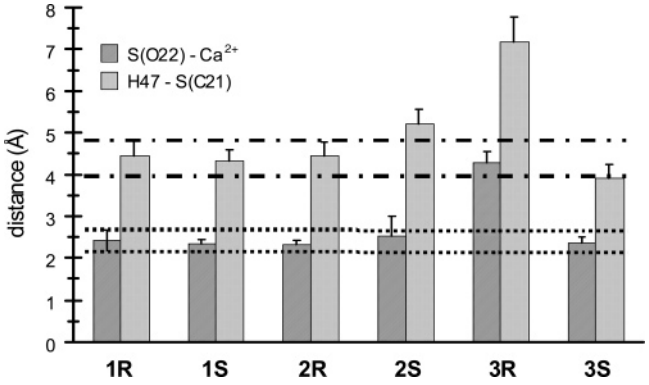

Figure 9. Average distances of His47(ND1)−S(C21) and S(O22)−Ca^{2+} extracted from the simulations of the different $sPLA_2$−phospholipid complexes. Averages and standard deviations (SDs) were calculated from a series of simulations of a particular complex, where only the last 5 ns of each simulation were used. The dashed-dotted and the dotted lines indicate the upper and lower errors of His47(ND1)−S(C21) and S(O22)−Ca^{2+} respectively extracted from the $sPLA_2$−**1R** simulations. Note, **1R** is the natural substrate for $sPLA_2$.

acts as the attacking nucleophile.[83−85] Figure 5 displays a schematic representation of the catalytic mechanism indicating that the calcium ion is coordinated by two carboxylate oxygen atoms of Asp48, by a backbone oxygen of Gly29, and two oxygens of the substrate.[83,84] The latter two coordinations involve a phosphate oxygen and the *sn*-2 carbonyl oxygen and serve as stabilization of the substrate. His47, which abstracts a proton from the incoming water molecule, is stabilized by Asp91 that additionally forms hydrogen bonds with Tyr51 and Tyr66. The oxyanion hole that stabilizes the transition state after nucleophilic attack is formed by the backbone HN group of Gly29 assisted by the charge of the calcium ion. In view of these interactions, we have monitored distances between Ca^{2+} and residues/atoms in $sPLA_2$ (Asp48(OD1), Asp48(OD2), and Gly29(O); Figure 6), distances that involve Asp91 or His47 (Asp91(OD1)−Tyr51(OH), Asp91(OD1)−Tyr66(OH), His47(HE2)−Asp91(OD1), and His47(ND1)−S(C21); Figure 7), and distances that involve the substrate (hereafter referred to as S) (S(O22)−Gly29(HN), S(O22)−Ca^{2+}, and S(O4)−Ca^{2+}; Figure 8). Atom types indicated in parentheses refer to the Protein Data Bank nomenclature, which will be used throughout. The time evolutions presented in Figures 6 to 8 are representative for all simulations.

Overall, coordinations of Ca^{2+} by Asp48 and Gly29 are rather stable (Figure 6). The increase of the Ca^{2+}−Asp48(OD1) distance taking place in concert with the change in Ca^{2+}−Gly29(O) and occurring over a relatively short time interval was also observed in some of the other simulations. In all cases, the fluctuations occurred only over a short time period and at different time intervals, and we conclude that there was no systematic pattern in these fluctuations. As discussed above, Asp91 forms hydrogen bonds with Tyr51, Tyr66, and His47 (Figure 7). The Asp91(OD2)−Tyr66(OH) distance is stable throughout the simulations, whereas distances between Asp91 and Tyr51 or His47 show larger fluctuations than those observed for Asp91−Tyr66. The distance change observed for His47−Asp91 between ∼1.8 ns and ∼6.1 ns corresponds to a reorientation of the histidine (180 degrees flip of the ring system), and hence, a similar change is observed for His47(ND1)−S(C21). After ∼6.1 ns, the His residue flips back in the orientation, where His47 can participate in hydrolysis. The flip-flop of His47 was only observed in a few simulations and encountered for shorter time periods than that shown in Figure 7. Substrate−Ca^{2+} distances are stable throughout the simulations (Figure 8), and Ca^{2+} binds tightly to the phosphate oxygen. Noticeable, the S(O22)−Gly29(HN) distance is stable but shows relatively large fluctuations.

Visualization of the time evolution of these distances is an important tool to study the stability of these interactions but provides no information of statistical significance. We have therefore calculated averages over time and configurational space (i.e., simulations) using the last 5 ns of each simulation. Before calculating the averages, all distances were checked if

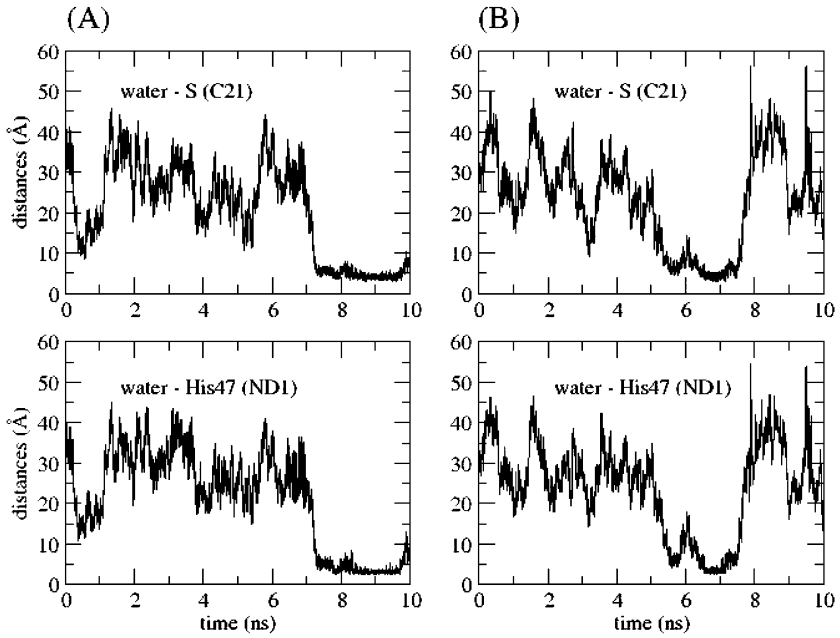

Figure 10. Trajectories of two water molecules (A and B) monitored in an $sPLA_2$−**1R** simulation. Distances are calculated with respect to S (C21) (top) and H47 (bottom).

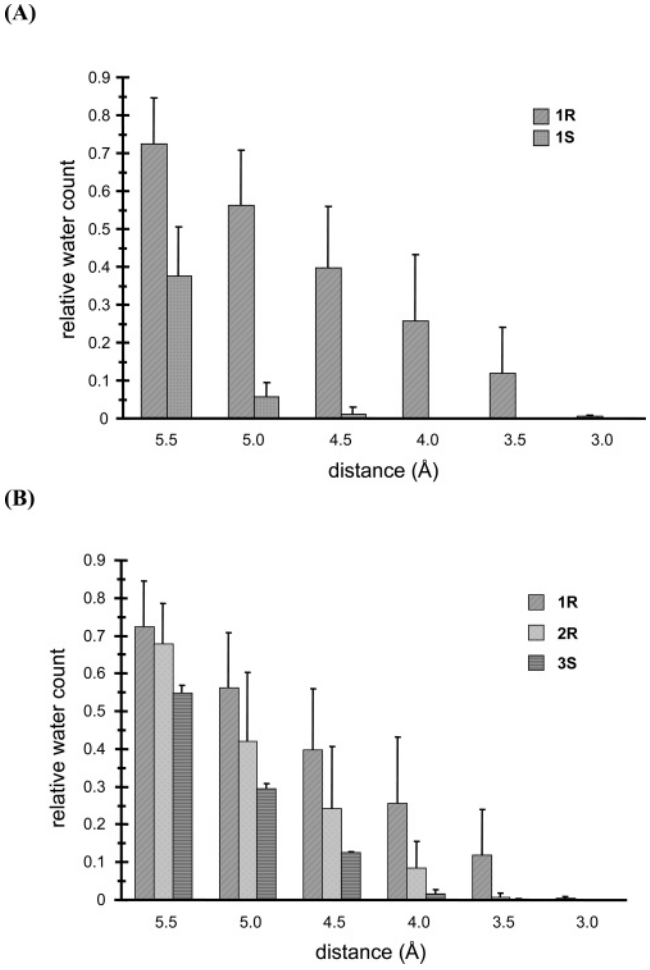

Figure 11. (A) Average relative water counts extracted from the **1R** and **1S** simulations. (B) Average relative water counts extracted from the **1R**, **2R**, and **3S** simulations. Before calculating the averages, the data extracted from each simulation were arbitrarily normalized by the water count at 6 Å of the simulation.

they were stable throughout the simulations. Overall, the distances are very stable, and differences in average distance between the different complexes are within the statistical uncertainties (a summary is provided as Supporting Information; Table S1). Relatively large variations are observed for His47-(ND1)−S(C21) and S(O22)−Ca^{2+} distances in the different complexes (Figure 9). Particularly, **2S** and **3R** have on average a larger His47(ND1)−S(C21) distance than that in the complex with the natural substrate (**1R**). This could explain the lack of $sPLA_2$ activity toward these phospholipids. The phospholipids are not perfectly aligned in the binding cleft of $sPLA_2$ to allow for hydrolysis to occur. Surprisingly, the distances monitored in $sPLA_2$−**1S** are (within the statistical uncertainties) the same as those in $sPLA_2$−**1R** (Figure 9, Table S1). The reasoning that **1S** is not a substrate for $sPLA_2$ (enzymatic hydrolysis is a stereospecific reaction) must depend on other factors. As discussed above, the enzymatic reaction requires that a water molecule acting as a nucleophile is positioned correctly relative to His 47(ND1) and the carbonyl carbon of the substrate (C21, Figure 5). If water molecules cannot reach this position, it might explain the lack of $sPLA_2$ activity.

Simulations - Nucleophilic Water Molecule. A prerequisite for catalysis is that a water molecule can come in close vicinity to His47(ND1) and S(C21). We therefore have monitored the movement of water molecules, and trajectories of two water molecules taken from a $sPLA_2$−**1R** simulation are shown in Figure 10. In order to quantify the positioning of the potential catalytic water molecules, we have measured the probability of water molecules being at a certain distance from both His47-(ND1) and S(C21), hereafter referred to *H*−*S*. We counted the number of water molecules that are within a certain distance from *H*−*S*. The diffusion of water molecules is governed mainly by thermal motion, and hence, water molecules randomly diffuse into the catalytic site.[82] Since this is a random event, relatively large differences are observed between a series of simulations of the same complex. We have therefore arbitrarily normalized each result from a particular complex simulation with the water count determined at 6.0 Å from *H*−*S* of the simulation. Average relative water counts for each series are provided in the Supporting Information (Table S2). Comparing **1R** with **1S** (Figure 11A) reveals that the lack of $sPLA_2$ activity toward **1S** is related to positioning of water molecules. Within the time frame of the simulations of **1S**, no water molecule could be detected within 4 Å of *H*−*S*, and the relative water count within 4.5 Å is much less than that found for **1R** (Figure 11A). Also clear differences are seen for **1R**, **2R**, and **3S** (Figure 11B). Independent of the distance analyzed, the relative water count follows the pattern **1R** > **2R** > **3S**. Within 4 Å of *H*−*S*, the relative water count decreases by ∼30% from **1R** to **2R** and an additional ∼25% from **2R** to **3S** implying that the $sPLA_2$ activity toward these phospholipids follows the same trend: **1R** > **2R** > **3S**. This observation is in good agreement with the experimental activity data.[62,67]

Conclusions

We have shown that unnatural phospholipid analogues where the head group (normally located at the *sn*-3 position) was placed at the 2-position are relatively good substrates for $sPLA_2$.[67] We therefore decided to carry out molecular dynamics simulations to understand on a molecular level why $sPLA_2$ can tolerate phospholipids with their head group in the 2-position and to explain the different $sPLA_2$ activity toward natural and unnatural phospholipid analogues. In the simulations of $sPLA_2$−**2S** and $sPLA_2$−**3R**, the distance between His47 and the carbonyl carbon (C21; Figure 5) of the substrate is larger than that observed in the simulations of $sPLA_2$−**1R** (natural substrate). The phospholipids cannot arrange in the right geometry in the binding cleft due to the additional space and are therefore not hydrolyzed by $sPLA_2$. Although the phospholipids **1R**, **2R**, and **3S** align perfectly in the binding cleft, these lipids are hydrolyzed by $sPLA_2$ with different efficiencies. Our simulations revealed that the difference observed in $sPLA_2$ activity is caused by less efficient access of water molecules to the active site. During the hydrolysis, a water molecule that acts as the nucleophile in the reaction is positioned between His47 and C21 (Figure 5). We have monitored the number of water molecules that enter the region between His and C21 for the different $sPLA_2$−phospholipid complexes and found that the probability of a water molecule reaching the correct position such that hydrolysis can occur is reduced for the unnatural phospholipids. The relative

(84) Janssen, M. J. W.; van de Wiel, W. A. E. C.; Beiboer, S. H. W.; van Kampen, M. D.; Verheij, H. M.; Slotboom, A. J.; Egmond, M. R. *Protein Eng.* **1999**, *12*, 497−503.
(85) Sekar, K.; Yu, B.-Z.; Rogers, J.; Lutton, J.; Liu, X.; Chen, X.; Tsai, M.-D.; Jain, M. K.; Sundaralingam, M. *Biochemistry* **1997**, *36*, 3104−3114.
(86) Zhou, F.; Schulten, K. *Proteins* **1996**, *25*, 12−27.

water count follows **1R** > **2R** > **3S**, which is in excellent agreement with experimentally determined activity data.[62,67]

Acknowledgment. Financial support from the Danish National Research foundation via a grant to the MEMPHYS-Center for Biomembrane Physics is acknowledged. Simulations were performed at the Danish Center for Scientific Computing at the University of Southern Denmark.

Supporting Information Available: Root-mean displacement as function of simulation time; time-averaged fluctuations of residues, averaged distances, and averaged relative water count. This material is available free of charge via the Internet at http://pubs.acs.org.

JA067755B